A&A 434, 613–621 (2005)
DOI: 10.1051/0004-6361:20042437

Astronomy & Astrophysics

Masers as signposts of high-mass protostars

A water maser survey of methanol maser sources⋆

M. Szymczak[1], T. Pillai[2], and K. M. Menten[2]

[1] Toruń Centre for Astronomy, Nicolaus Copernicus University, Gagarina 11, 87100 Toruń, Poland
e-mail: msz@astro.uni.torun.pl
[2] Max-Planck-Institut für Radioastronomie, Auf dem Hügel 69, 53121 Bonn, Germany

Received 26 November 2004 / Accepted 31 December 2004

Abstract. The 22 GHz H_2O maser line was observed towards 79 candidate high-mass protostellar objects from a flux-limited sample of 6.7 GHz methanol sources. The emission was detected in 41 sources, towards 28 of these for the first time. The detection rate of 52% was similar to rates reported for other samples of high-mass protostars selected mainly with far-infrared (FIR) colour criteria. The median value of H_2O maser luminosity of $10^{-5.5}$ $L_\odot$ is equal to that of the CH_3OH maser luminosity, whereas the median OH maser luminosity was found to be ∼1.5 orders of magnitude lower. Comparison of the velocity ranges showing maser emission implies that for the majority of sources the H_2O and CH_3OH maser lines originate from different regions. The percentage of sources with emission in two or three of the maser species, their association with radio continuum and IR emission and the maser and IR luminosities are consistent with the view that evolutionary phases with H_2O and CH_3OH masers largely overlap and precede the OH maser phase, while at a later stage OH and CH_3OH masers may coexist. Strong correlations of OH and CH_3OH maser luminosities with IR luminosity and only a marginal correlation of H_2O and IR luminosity confirm current pumping schemes of all three maser lines.

Key words. masers – stars: formation – ISM: molecules – radio lines: ISM – HII regions

1. Introduction

It has been established that the physical conditions in massive star-forming regions favour maser emission from the water (H_2O), hydroxyl (OH), and methanol (CH_3OH) molecules (e.g. Kurtz et al. 2000; Reid & Moran 1988), although the different maser species probe varying temperature, density and chemical regimes (Menten 1996, for a brief review).

The 22 GHz transition of H_2O is one of the best known and most widespread tracers of extremely young and heavily embedded low- and high-mass stars. Several single dish surveys of H_2O masers were carried out towards known ultracompact HII regions (UCHIIRs) and UCHIIR candidates selected on the basis of their IRAS colours (Wouterloot & Walmsley 1986; Churchwell et al. 1990; Palla et al. 1991, 1993; Codella et al. 1995, 1996) and also towards what Sridharan et al. (2002) and Beuther et al. (2002) identify as high-mass protostellar objects (HMPOs), i.e. sources with the same colours as UCHIIRs but with little or no radio emission. In these surveys detection rates were frequently high (up to 67%) but strongly dependent on the sensitivity of the observations and selection criteria.

From the observations over the last decade, it has become clear that H_2O maser emission marks the earliest stages of high-mass star formation and, more specifically, arises in outflows from young stellar objects (Menten 1996).

High-mass star forming regions frequently display methanol maser emission. Several hundreds of methanol masers were detected towards UCHIIR candidates selected with the IRAS colour criteria of Wood & Churchwell (1989, hereafter WC89) or other less stringent criteria (Menten 1991; Schutte et al. 1993; van der Walt et al. 1995, 1996; Walsh et al. 1997; Slysh et al. 1999; Szymczak et al. 2000) as well as in unbiased surveys of selected areas of the Galactic plane (Caswell 1996; Ellingsen et al. 1996; Szymczak et al. 2002).

These studies have shown that almost all UCHIIR candidates with extremely red IRAS colours are methanol sources, suggesting that methanol masers are closely associated with the earliest stage of high-mass star formation, in many cases with a stage preceding the formation of an UCHIIR.

Few studies have examined the relationship between H_2O and CH_3OH masers in the same samples of high-mass protostar candidates; see papers by Codella & Moscadelli (2000) and Beuther et al. (2002). The detection rate of Codella & Moscadelli (2000) was ∼22% for both species, but only 40% of the H_2O sources had a CH_3OH counterpart, indicating that at least a substantial number of sources is either in an H_2O maser-*or* a CH_3OH maser bearing-phase. The formation of H_2O and CH_3OH masers in identical environments is precluded by very

⋆ Table 3 is only available in electronic form at the CDS via anonymous ftp to cdsarc.u-strasbg.fr (130.79.128.5) or via http://cdsweb.u-strasbg.fr/cgi-bin/qcat?J/A+A/434/613

different excitation requirements; for H_2O masers collisional pumping occurs in shocks at the interface between the outflowing material and the surrounding molecular gas (e.g. Elitzur et al. 1989), while for CH_3OH masers radiative pumping (possibly) in circumstellar discs is proposed at much lower temperatures and densities (e.g. Cragg et al. 2002).

This view is confirmed by high resolution observations, which do not show spatial correlation between the two maser species in detail (on a ∼sub few thousand AU scale, Forster & Caswell 1989), although in regions harbouring masers in both species these are found within 0.15 pc of the exciting source, if the latter is directly detected at all (Beuther et al. 2002).

In this paper we present the results of H_2O maser observations of a homogeneous and unbiased sample of 6.7 GHz CH_3OH maser sources. The sample was obtained from a blind survey of the Galactic plane in the longitude range 20°−40° and latitude range from −0.°52 to 0.°52 (Szymczak et al. 2002). We note that the sample is flux-limited and does not suffer from other factors such as incompleteness or confusion of IR surveys and uncertainties of selection criteria, which usually affected other samples. The whole sample was recently searched for all four OH transitions at 1.6 GHz (Szymczak & Gérard 2004).

This study continues our attempts at better characterizing the properties of the sample selected on the basis of showing 6.7 GHz methanol maser emission. For the reasons mentioned above, high angular resolution data are needed to study the association between H_2O and CH_3OH masers in individual target sources. Nevertheless, our homogeneous and large data set, although taken at low angular resolution, allows for meaningful statistical analyses of maser kinematics (via LSR velocities and velocity ranges) and luminosities. Moreover, we emphasize the "signpost effect": wherever there is a maser, there must be an exciting source. High resolution follow-up studies at radio, millimeter and infrared wavelengths will reveal these sources' properties. Our detections provide a source list for future high resolution studies.

2. Observations and results

2.1. Observations

We observed the $6_{16} \rightarrow 5_{23}$ (22 235.0798 MHz) transition of H_2O on 2003 August 12−15 and 19 with the Effelsberg 100 m telescope. The half-power beam width was 40″. During the observations the system temperature varied between 60 and 150 K around a median value of 92 K. The spectrometer was split into two banks of 4096 channels, each of which was used. The bandwidth of 20 MHz was centred on the centroid of the CH_3OH velocity interval (Szymczak et al. 2002), giving an effective velocity coverage of ∼260 km s^{-1} and a spectral resolution of 0.066 km s^{-1}. The radial velocities were measured with respect to the local standard of rest (LSR). The observations were made in the position switching mode and resulted in a mean rms noise value of 0.45 Jy in the spectra. The calibration is estimated to be uncertain by ∼30%.

We searched for the H_2O line towards 79 targets from a sample of CH_3OH masers found in the unbiased survey of the Galactic plane for the 6.7 GHz methanol line (Szymczak et al. 2002).

Table 1. 22 GHz line parameters for the new detections.

Source (l, b)	ΔV	V_c	V_p	S_p	S_i
	(km s^{-1})			(Jy)	(Jy km s^{-1})
20.24+0.07	1.1		57.3	1.7	1.3
21.57−0.03			99.0	1.6	1.1
22.05+0.22			53.4	2.5	0.8
23.19−0.38	2.6	78.5	78.1	31.9	22.1
23.26−0.24	5.1	57.1	55.3	2.3	2.8
23.39+0.19	2.1		72.0	3.3	3.5
23.97−0.11	42.8	52.4	32.8	8.8	14.2
24.33+0.14	54.5	85.5	61.7	7.4	39.6
24.53+0.32	7.1	106.0	103.3	5.5	6.2
24.93+0.08			47.7	1.1	1.3
25.71+0.04			63.4	1.2	0.7
25.83−0.18	56.4	94.7	94.9	338.	754.
27.21+0.26			18.6	4.1	5.9
27.36−0.16	16.5	89.5	95.7	50.6	121.
27.78+0.07	33.1	85.2	69.6	1.1	2.3
28.19−0.05	7.4	92.7	90.7	7.1	15.6
28.40+0.07			40.1	2.6	2.6
28.82+0.37	7.3	86.8	87.2	81.5	93.4
28.85+0.50	5.5	87.3	86.9	12.2	29.4
30.31+0.07	4.3	46.6	47.9	5.6	9.3
30.70−0.07	46.7	76.2	54.7	1.9	10.8
30.78+0.23	7.6	62.9	39.1	0.5	1.7
30.79+0.20	12.4	70.8	72.0	5.5	7.7
33.64−0.21			56.4	1.2	1.5
36.11+0.55	10.1	76.7	72.4	2.5	5.0
37.47−0.11	3.8	61.7	56.7	3.6	5.5
37.60+0.42	11.1	86.3	90.2	1.1	5.8
39.10+0.48	7.2	27.0	24.4	1.2	3.5

2.2. New detections

The 22 GHz maser line was detected in 41 sources, 28 of which are new detections. The basic parameters of the new detections and previously known masers, determined from Gaussian fitting, are summarized in Tables 1 and 2, respectively. The source designation in galactic coordinates, the velocity range of emission (ΔV), the velocity centre between the extremes (V_c), the velocity of peak emission (V_p), the flux densities of peak (S_p) and of integrated emission (S_i) are given. The same definitions hold for all types of maser observations discussed in the paper. The spectra of newly detected and previously known masers are shown in Figs. 1 and 2, respectively. Hanning smoothing was only applied to noisy spectra and reduced the resolution by a factor of 2.

Most of the new detections are relatively weak, frequently only showing a single narrow feature. There are only three sources with a peak flux density higher than 50 Jy. Four sources have maser emission over a velocity range larger than 40 km s^{-1}.

Table 2. 22 GHz line parameters for previously known masers.

Source (l, b)	ΔV	V_c	V_p	S_p	S_i
	(km s^{-1})			(Jy)	(Jy km s^{-1})
20.08−0.14	15.6	24.7	23.6	18.8	46.4
21.87+0.01	4.4	22.3	23.2	7.0	12.6
22.35+0.06			88.3	3.6	3.1
23.01−0.41	26.0	79.5	77.0	206.0	534.6
23.44−0.18			96.4	11.0	12.2
24.79+0.09	94.0	80.0	112.3	413.0	1575.2
27.28+0.15			31.2	6.7	5.2
29.95−0.02	30.8	95.4	99.3	27.6	148.1
30.59−0.04	72.0	9.0	21.3	1.0	3.6
30.76−0.05	27.0	80.5	87.1	1.0	5.2
30.82−0.05	71.0	93.5	101.4	169.0	250.2
33.13−0.09			68.7	1.6	2.0
37.55+0.19			89.1	1.0	1.5

2.3. Data summary

The properties of our 79 targets derived from the present observations and other data available in the literature are summarized in Table 3. The kinematic distances have been determined from the central velocities of the 6.7 GHz masers as measured by Szymczak et al. (2002) and the expression for the Galactic rotation curve given by Brand & Blitz (1993). The centre velocity, V_c, of the methanol line is a reliable estimator of the systemic velocity, since it usually coincides with the velocity of CS emission (Bronfman et al. 1996), tracing dense gas, to within 4 km s^{-1} (Szymczak & Gérard 2004). The sources are within the solar circle, so there are two solutions for the kinematic distances. For a few objects, unambiguous distances were taken from the literature.

The isotropic maser luminosities of the three maser molecules are derived. The OH maser luminosity was obtained using the sum of integrated flux densities of the 1665 and 1667 MHz lines (Szymczak & Gérard 2004). These main lines dominate in the studied sources, whereas the satellite lines at 1612 and 1720 MHz are rarely seen and, if seen at all, relatively weak; therefore their contributions are ignored. The luminosity of the methanol maser emission was inferred from the integrated flux density in the 6.7 GHz line (Szymczak et al. 2002).

The present observations are used to derive the water maser luminosity for 41 targets. Assuming that with our sensitivity we are able to detect a maser feature of velocity width of 1 km s^{-1} our luminosity upper limit is 2.6×10^{-22} W m^{-2}, which corresponds to $10^{-6.7}$ $L_\odot$ for source at 5 kpc. H_2O masers in 25.40+0.11, 26.59−0.01, and tentatively 30.82+0.27, were recently discovered with the same instrument and similar sensitivity (Sridharan et al. 2002) and 37.53−0.11 by Hofner & Churchwell (1996). These four objects were not detected in the present study. Assuming "equivalent" velocity range of 1.5 km s^{-1} for all four objects we estimate upper limits on the ratio of the luminosities derived in the previous studies and our observations of 12.7, 6.1, 1.7, and 6.8, respectively.

Flux density variations of that order are commonly seen in water masers (Brand et al. 2003). Although detailed analysis of the variability of the H_2O sources is beyond the scope of the present paper, we note similar ratios among 13 known sources in the sample. We found the highest change (increase) in the integrated flux density by a factor of 37 in 23.01−0.41 as compared to data taken at epoch 1992.99 (Valdettaro et al. 2001).

The shape of most of the spectra also exhibit substantial changes. For instance the 27.28+0.15 maser was previously detected at −22.5 km s^{-1} with a peak flux density of ∼0.4 Jy (Churchwell et al. 1990) while we detected only a new feature of a 5.9 Jy peak flux density at 31.2 km s^{-1}.

To determine the IR luminosity, we identified candidate IRAS source counterparts to within 1′ from the methanol position (Szymczak et al. 2002). We then estimated the total IR flux using the relation given by Walsh et al. (1997) (their Eq. (3)) adopting the same factor $Y = 0.6$ to incorporate the flux from outside the IRAS wavelength range.

Radio continuum counterparts of our targets were identified within 1′ from the methanol position using mainly the VLA 5 GHz catalogue of UCHIIRs (Becker et al. 1994). Sources with radio continuum emission are marked in the last column of Table 3.

3. Discussion

3.1. Detection statistics

H_2O masers were detected in 52% (41/79) of the sources in our CH_3OH sample (Table 3). Sridharan et al. (2002) reported a detection rate of 42% for their sample of 69 high-mass protostellar objects, which are basically bright IRAS point sources with colours typical of UCHIIRs with detected CS emission and without significant radio emission at 5 GHz. They carried out the observations with the same instrument and sensitivity as we. Our sample has only three sources in common with that of Sridharan et al. It appears that the detection rates for both samples do not differ significantly. However, the real difference in the detection rates might be larger and our value should be regarded as a lower limit, since the errors on our methanol positions of about 30″ for strong sources and as large as 70″ for weak sources (Szymczak et al. 2002) are comparable to or larger than the 40″ beamwidth of our H_2O observation: we simply may have missed sources. As we did not make raster mapping to find peak position our integrated flux density estimates may by quite uncertain as well (see Sect. 3.3).

Sridharan et al. used the IRAS positions, and consequently their data do not suffer as much from that effect, although many IRAS positions have uncertainties >10″. In our sample we note a considerable decrease of the H_2O maser detection rate for the sources with weak methanol emission. This can be due to inaccurate positions of methanol sources. However, it could be also related to a correlation of luminosities of both maser lines (see Sect. 3.3). Finally, variability may play a role, which is difficult to quantify.

Churchwell et al. (1990) detected H_2O masers in 67% of 84 IRAS colour-selected UCHIIRs showing radio continuum emission. The sensitivity of their observations was about

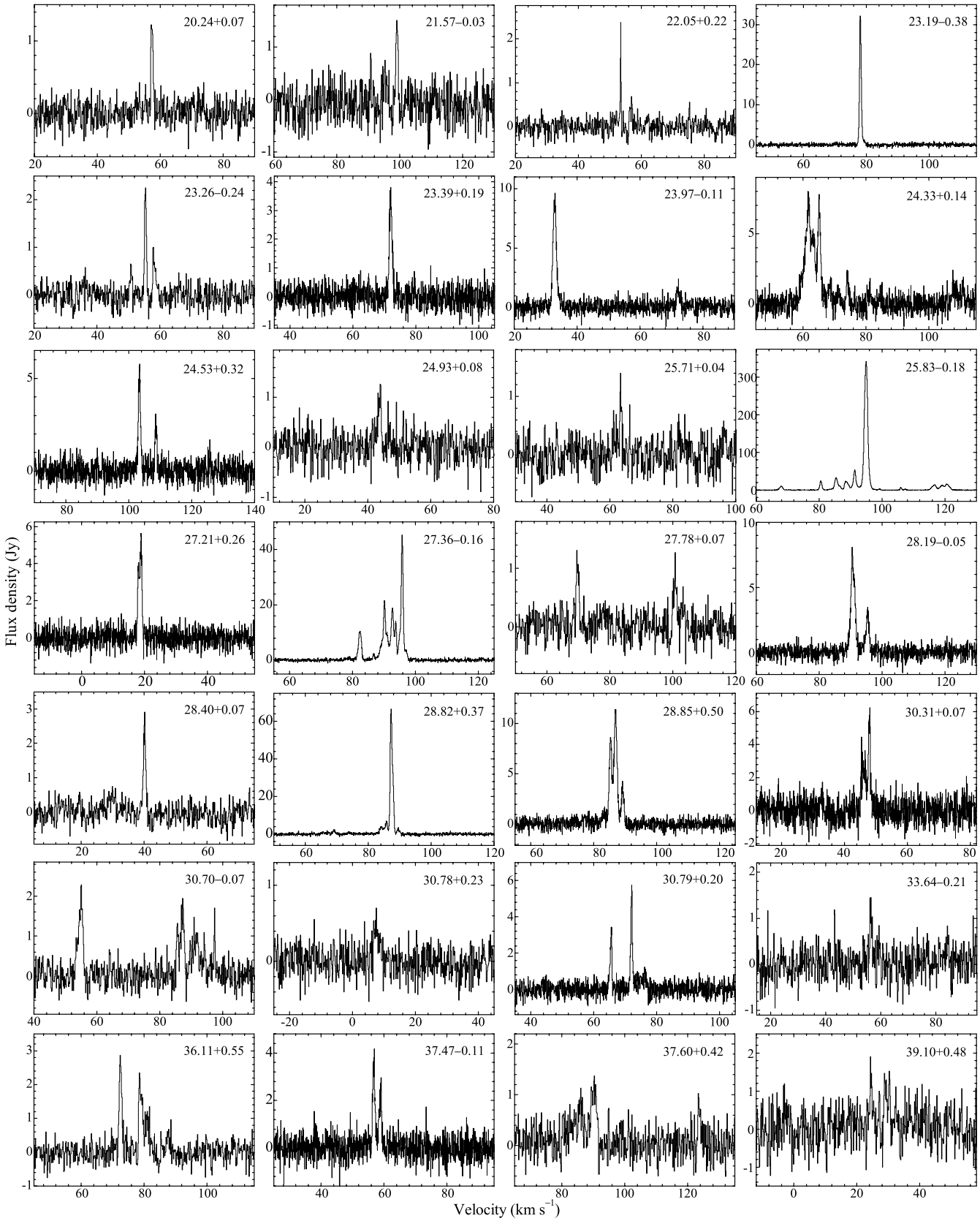

Fig. 1. Spectra of the newly detected water masers.

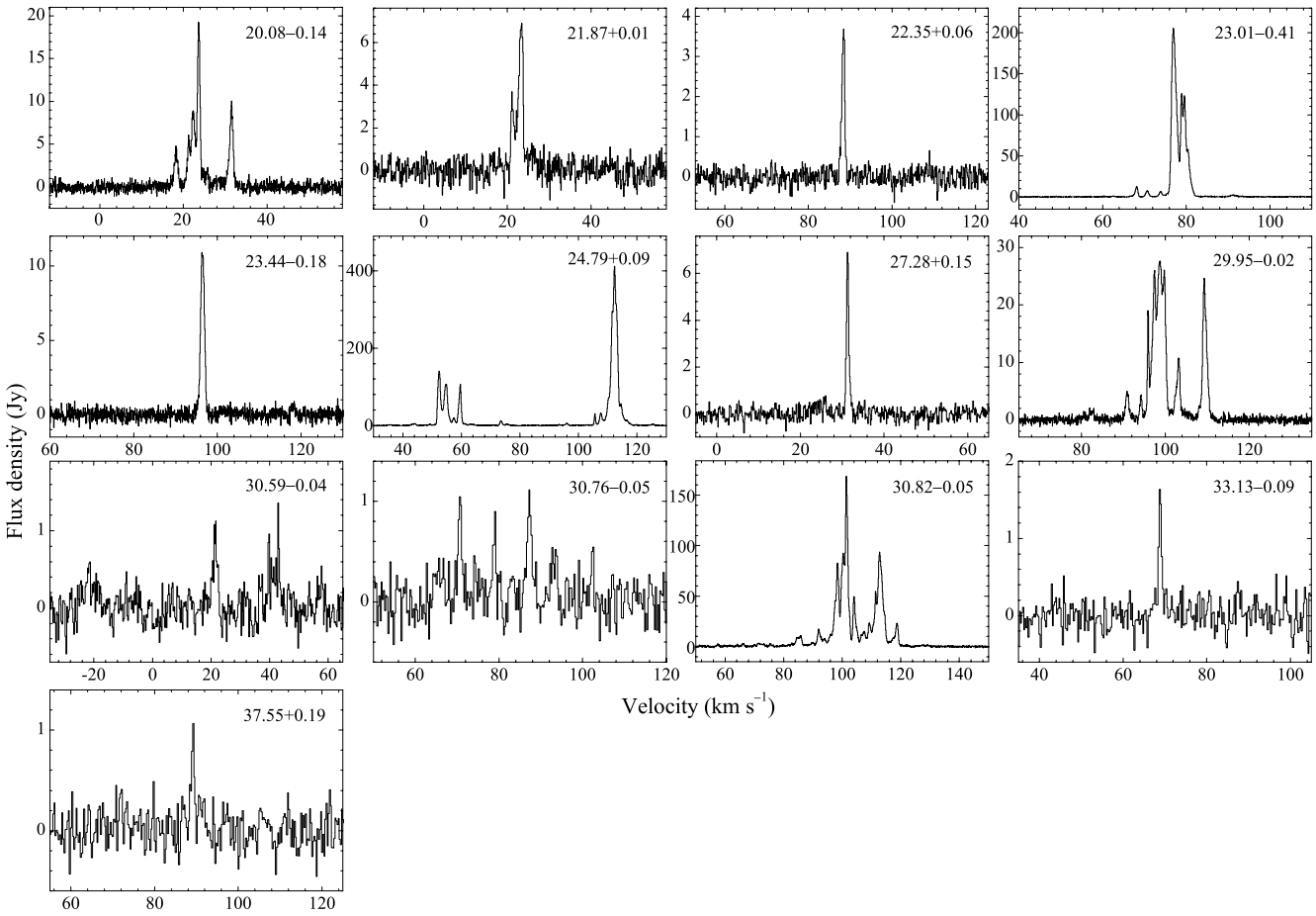

Fig. 2. Spectra of previously known water masers.

a factor of 2.7 better than ours. When scaled to the sensitivity of our observations their detection rate is reduced to 53%, which is in excellent agreement with the present detection rate. We note that Churchwell et al.'s sample is largely independent from ours, with only 7 objects in common. Therefore, it is very likely that both samples probe the same population of objects with a high probability of the occurrence of H_2O maser emission. Palla et al. (1991) investigated the H_2O maser properties of a sample of 260 bright IRAS objects. For about half of their sources (125), which satisfied the WC89 colour criteria, the detection rate was 26%. We note that in our survey there is a large number of maser sources well below their detection limit (3σ) of about 5 Jy.

When our data are scaled to their sensitivity the detection rate would decrease to 25%. Thus for both samples the percentage of H_2O masers is nearly the same. We conclude that the percentage of H_2O masers in the unbiased sample of methanol sources is nearly the same as that reported for the above three largely independent samples of high-mass protostar candidates selected by different criteria. The 6.7 GHz methanol maser line is as powerful a tool to probe high-mass star forming regions and identify high-mass protostars as methods based on far-infrared, radio continuum, and thermal line data (WC89; Sridharan et al. 2002).

Water maser emission generally exhibits strong flux variations (e.g. Brand et al. 2003), which can influence the detection rate. It is very likely that the four known sources mentioned in Sect. 2.3 were not detected due to variability. This implies that the detection rate can vary by 5−6%.

We suspect that the number of H_2O masers in the sample detected at least at some epochs could be increased if not detected sources were reobserved.

3.1.1. Sources with masers in different species

With the completion of the present survey we possess data for the three major maser species for a medium-size sample of objects. This allows us to deduce information on the occurrence or non-occurrence of maser emission in different species.

To do this we applied a common sensitivity of 1.6 Jy, which is a cut-off level for the unbiased CH_3OH survey (Szymczak et al. 2002), for OH data (Szymczak & Gérard 2004) and the present H_2O observations. Table 4 summarizes the number and percentage of sources with masers from more then one species together with radio and IRAS properties.

The percentage of sources with both methanol and water masers (44%) in our sample is larger than the 29% in Sridharan et al.'s (2002) sample. However, for their subsample of 29 objects observed with a few arcsecond resolution this percentage is 56% (Beuther et al. 2002). Codella & Moscadelli (2000) found that about 40% of H_2O masers associated with UCHIIRs

Table 4. Statistics on the overlap of maser species, radio continuum emission and IRAS emission. The third column gives the percentage of sources with masers in two or three of the maser species (OH, H_2O, and CH_3OH) with respect to the total number of sources studied (79). The fifth and seventh columns are the percentages of radio and IRAS counterparts, respectively, with respect to the number of maser sources given in the second column.

Overlap	$N_{\rm maser}$	%	$N_{\rm radio}$	%	$N_{\rm IRAS}$	%
$OH/CH_3OH/H_2O$	9	11	4	44	5	56
OH/CH_3OH	12	15	4	33	4	33
CH_3OH/H_2O	26	33	10	38	14	54
CH_3OH	32	41	6	19	18	56

with detected radio continuum emission have CH_3OH counterparts.

Although association of both maser species in the sample might be partly caused by insufficient angular resolution we notice a high fraction of sources showing both CH_3OH and H_2O emission. As this fraction is comparable to that reported for the above mentioned samples we suggest that CH_3OH maser efficiently probes the same population of high mass star-forming regions as do far infrared colour criteria (WC89). In the same population, evolutionary phases in which, both, CH_3OH and H_2O emission is produced, can overlap significantly (Codella & Moscadelli 2000) and both masers likely originate in similar environments, although the *phenomena* actually producing the maser emission may be quite different – warm, moderately dense gas for CH_3OH and hot, shocked, dense gas for H_2O (Menten 1996). Masers from different species may arise from different young stellar objects within the same protostellar cluster. The correlations discussed in the following sections should be interpreted only as presence of a given maser type in the star-forming complex during its evolution.

Forster & Caswell (1989) established that OH and H_2O masers closely associate in compact groups of size of ~0.03 pc, whereas in more extended groups (~0.15 pc) are spatially intermixed but usually do not coincide. They propose a scenario that close OH/H_2O associations last about 10^5 yr during an accretion phase. When accretion terminates OH/H_2O groups expand over the next 10^4 yr and then disappear. Caswell et al. (1995) showed that OH and CH_3OH masers are very closely associated and generally occur near a common energy source.

A view of the W3(OH) region (Menten 1996) provides lessons applicable here. OH and CH_3OH, but *no* H_2O maser emission is observed towards half of the ultracompact (size ≈ 2000 AU) HII region radio emission. In contrast, very intense H_2O maser emission is observed towards a separate protostar or cluster of protostars 0.06 pc (or 6″) away, which also gives rise to strong *thermal* molecular and dust emission (Wyrowski et al. 1999). At the resolution of the IRAS satellite these sources cannot be separated. Needless to say, with our coarse resolution, in particular at 6.7 GHz, H_2O and CH_3OH masers would appear as coextensive.

The probability of finding an OH maser counterpart of a CH_3OH/H_2O maser source is relatively low (Table 4). This may suggest less overlap of their evolutionary phases as compared to overlap of the CH_3OH and H_2O maser phases. Further arguments supporting this suggestion are presented in Sect. 3.3.

3.1.2. Association with radio and IRAS sources

Out of 79 sources, 24 (30%) are associated with radio continuum emission (Tables 3 and 4). This percentage may be an overestimate, again, due to the relatively high uncertainty of the methanol positions. From high resolution data, Walsh et al. (1998) derive that only 20% of methanol masers are accompanied by radio continuum. Beuther et al. (2002) found continuum emission at centimeter wavelengths in about 31% of sources with CH_3OH and H_2O masers. The presence of radio continuum is thought to be a signpost of high-mass stars that have recently ignited and should, thus, indicate more evolved objects. Therefore, a prevalence of CH_3OH and H_2O masers without detectable radio continuum emission, in the three almost independent samples of high mass protostar candidates, implies that most of them are in the earliest stages of evolution.

Alternatively, some of the objects may be associated with less massive stars where the ionization rates are too low to produce observable UCHIIRs. The latter possibility is less probable as generally no methanol emission was detected towards low-mass young stellar objects (Minier et al. 2003), whereas such objects frequently show very intense H_2O maser emission (e.g. Valdettaro et al. 2001). Objects with only CH_3OH maser emission (Table 4) have the lowest percentage of radio counterparts (19%). This seems to be consistent with Beuther et al.'s (2002) result and may suggest that due to the ignition of the central object the CH_3OH maser emission ceases before the H_2O maser emission. However, there are well-known counter examples, perhaps most prominently W3(OH) discussed above.

There are only two sources 24.51−0.05 and 28.31−0.40 with only OH maser and radio emission. We cannot state, however, that they are more evolved than other our targets. More than 50% of the sources are associated with an IRAS point source (Table 4).

This is consistent with results reported by Ellingsen et al. (1996) and Beuther et al. (2002). The percentage of methanol sources associated with mid-infrared emission (MIR) is ~70% (Walsh et al. 2001) as IRAS point sources do not always coincide with the MIR sources possibly due to significant confusion.

3.2. Velocities

The distributions of velocity ranges of OH and CH_3OH masers in the sample do not differ (Fig. 3); the averages are 8.0 ± 0.7 and 8.6 ± 0.5 km s^{-1}, respectively. ΔV of these masers is never larger than 20 km s^{-1}. In contrast, out of 45 H_2O sources 33% have ΔV larger than 20 km s^{-1} while in 22% of sources its value exceeds 40 km s^{-1}. This suggests that at least one third of the water masers in the sample originate from environments different than the methanol masers and some of them can be associated with outflows or jets.

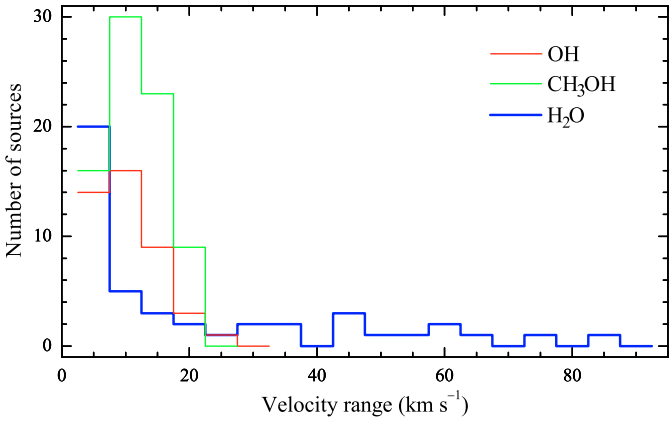

Fig. 3. Histograms of the velocity extent of three maser lines.

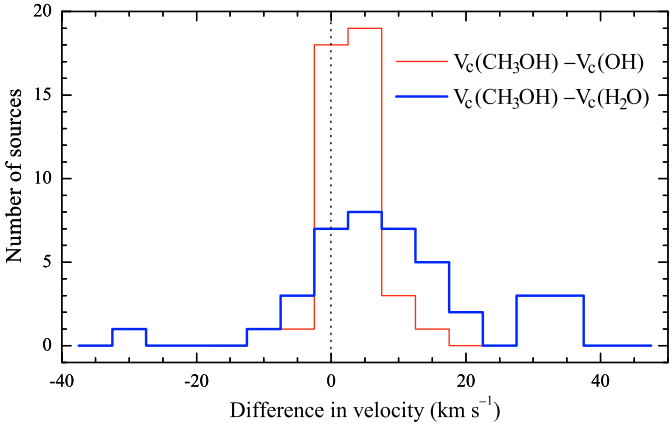

Fig. 4. Histograms of the difference in the centroid of the velocity maser intervals.

The distributions of the difference in V_c between CH_3OH and OH and between CH_3OH and H_2O are shown in Fig. 4. Out of 43 OH masers, 88% have velocity differences smaller than 5 km s^{-1}. Among H_2O masers, about 61% have velocity differences less than 10 km s^{-1} and 37% have differences less than 5 km s^{-1}. The small velocity difference between CH_3OH and OH implies that the maser lines of both molecules emerge either from the same regions of material surrounding the central object or from different clumps which are not strongly perturbed by the neutral shocks. This interpretation is consistent with high angular resolution observations of W3(OH) (Menten et al. 1992), where the distribution of the 6.7 GHz methanol masers follows closely that of the 1665 MHz OH masers.

Figure 4 implies that the majority of the H_2O masers originate in regions of velocities considerably different from the methanol velocities. As already discussed above, high resolution data indicate that there are clear spatial separations between both maser types (Beuther et al. 2002). Moreover, the velocity differences can reflect different excitation conditions. The excitation of H_2O maser is due to collisions with H_2 molecules within shocks associated with outflows or accretion (e.g. Elitzur et al. 1989) and requires densities, n, of $\sim 10^9$ cm^{-3} and temperatures, T, of ~400 K.

Radiative pumping in dense circumstellar gas (e.g. discs) is favoured for CH_3OH masers (e.g. Cragg et al. 2002, find

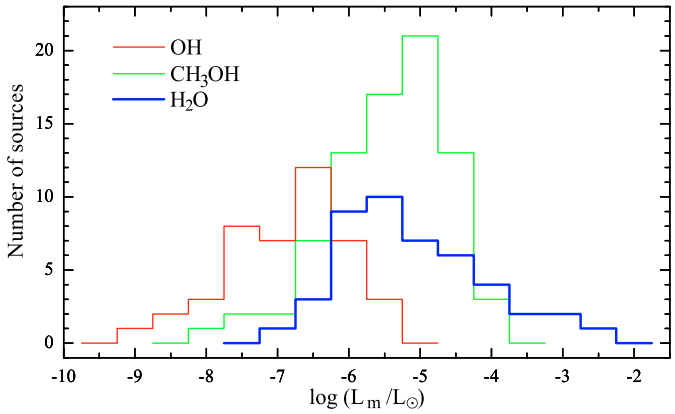

Fig. 5. Histograms of the maser luminosity for three species assuming the near kinematic distance.

$n = 10^5$–10^8 cm^{-3} and $T \approx 100$ K). The distributions in Fig. 4 are shifted to positive values; the centroids of the OH and H_2O maser velocity intervals are generally blue-shifted relative to the centroids of the methanol velocity intervals being good estimates of the systemic velocities if one assumes that CH_3OH masers originate in discs. If all three lines are associated with the same central object, this shift implies that OH and H_2O masers are seen preferentially in front of the central object. CH_3OH masers are likely confined to the innermost dense parts of the environment of a high-mass star, while OH originates in less dense outer clouds and H_2O marks the high velocity part of outflows (Codella et al. 2004). The prevalence of the blue-shifted methanol maser emission may indicate that it arises from infalling gas.

3.3. Luminosities

Although the near-far kinematic distance ambiguity was largely not resolved, near kinematic distance are more likely for a large number of the sources listed in Table 3 (Churchwell et al. 1990; Walsh et al. 1997). The luminosity distributions for the three maser species shown in Fig. 5 were derived assuming the near kinematic distances. The median luminosity of H_2O masers is $10^{-5.5}$ $L_\odot$ and equals that of CH_3OH masers.

The H_2O luminosity distribution is clearly skewed to larger values, whereas that of the CH_3OH masers is skewed to smaller values, resulting in average luminosities of $10^{-5.3}$ and $10^{-5.7}$ $L_\odot$, respectively. There is no statistically significant difference between the luminosities of H_2O and CH_3OH masers. The average OH luminosity is $10^{-7.1}$ $L_\odot$. We state that while the luminosities of H_2O and CH_3OH masers are comparable, OH masers are less luminous by about 1.5 orders of magnitude. Because we did not make raster maps to find peak positions, our estimate of H_2O luminosity may be underestimated. In order to estimate this effect we compared our flux densities of 13 previously known sources with those published in the literature. The mean of ratios of our measurements and other authors' is 8.2 ± 16.0.

Distributions of the H_2O maser luminosity for the present sample and that of Sridharan et al. (2002) are shown in Fig. 6. No significant difference is seen between the samples.

Table 5. The average maser and IR luminosities.

Overlap	N_{maser}	$\log(L_{OH})$	$\log(L_{CH_3OH})$	$\log(L_{H_2O})$	N_{IR}	$\log(L_{IR})$
$OH/CH_3OH/H_2O$	9	-6.32 ± 0.14	-5.44 ± 0.32	-4.72 ± 0.44	5	4.62 ± 0.20
OH/CH_3OH	12	-6.72 ± 0.22	-5.29 ± 0.24		4	5.12 ± 0.25
CH_3OH/H_2O	26		-5.60 ± 0.15	-5.32 ± 0.19	14	4.61 ± 0.19
CH_3OH	32		-5.94 ± 0.13		18	3.76 ± 0.19

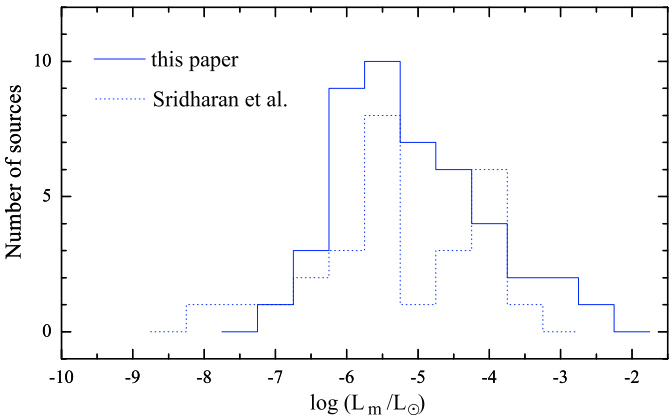

Fig. 6. Histograms of the H_2O maser luminosity for our sample and that of Sridharan et al. (2002).

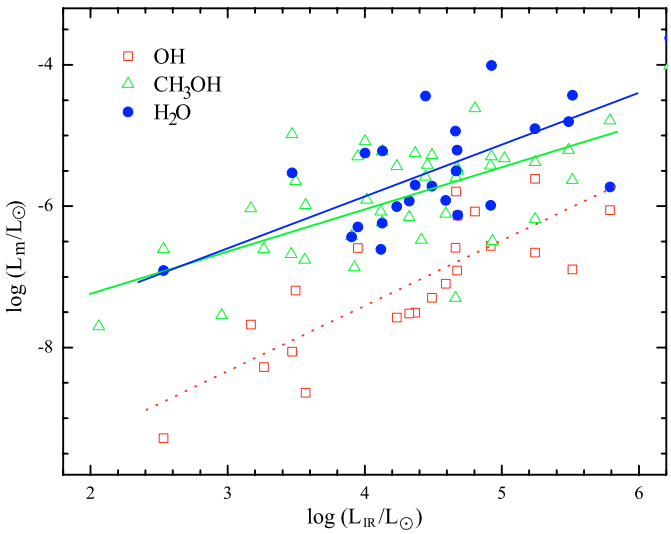

Fig. 7. Maser luminosities versus infrared luminosity. The least squares fits to the data are shown by dashed (red), thin (green) and thick (blue) lines for OH, CH_3OH and H_2O sources, respectively.

The median value of L_{H_2O} of Sridharan et al.'s sample is $10^{-5.6}$ $L_\odot$, which is essentially the same as our value. This suggests that the two samples probe similar population of young stellar objects and that our observations did not seriously underestimate the H_2O luminosities. However, more precise observations are needed to confirm this.

For the subsets of sources described in Sect. 3.1.1 (Table 4) the average maser luminosities are given in Table 5. We found for the subset of $OH/CH_3OH/H_2O$ sources the OH luminosity to be statistically significantly lower than the CH_3OH ($p < 0.02$) and H_2O ($p < 0.003$) luminosities, respectively. A strong difference in maser luminosities is also seen in the subset of OH/CH_3OH objects ($p < 0.0003$). The CH_3OH luminosity significantly differs between the OH/CH_3OH and CH_3OH maser groups. We conclude that the H_2O and CH_3OH maser luminosities are comparable within the error ranges, while the OH luminosity is always lower than the luminosities of the two other maser species. Models predict that OH and CH_3OH masers operate simultaneously under a wide range of physical conditions (Cragg et al. 2002). Our findings, on the other hand, suggest that OH maser emission appears in evolutionary phase later than CH_3OH and H_2O maser emission.

This is consistent with predictions of chemical models (Charnley et al. 1995; Charnley 1997). On the other hand if the luminosity ratio of OH and CH_3OH masers is constant then one would detect very weak OH masers associated with the subset of sources with CH_3OH masers of low luminosity. Such weak OH masers would be below the detection limit of the OH data available to us.

The subset of sources with CH_3OH alone has a significantly lower IR luminosity than that of the other subsets. The same trend is observed for the maser luminosity. As shown in Sect. 3.1.2 this group of objects is rarely associated with detectable radio continuum emission. We suggest that a significant fraction of the sources with only methanol maser emission, constituting more than 40% of the sample, precede in evolution those high-mass star forming sites associated with OH and UCHIIRs and some of them may be at very early stages.

Figure 7 shows the luminosities of three maser species versus the IR luminosity. The strongest correlation is seen for OH masers ($r = 0.84$, $p < 0.0001$). CH_3OH luminosity is also correlated with IR luminosity ($r = 0.55$, $p < 0.0001$). However, H_2O and IR luminosities are only marginally correlated ($r = 0.50$, $p < 0.04$). A tight dependence of OH and CH_3OH luminosities on IR luminosity does not necessarely imply that IR photons are involved in their pumping. It reflects rather the fact that more luminous star forming complexes provide more energy for the maser pumping. A correlation of H_2O luminosity with IR widely reported in the past (e.g. Wouterloot & Walmsley 1986; Palla et al. 1991) is not confirmed in our study. This may imply that IR photons do not influence H_2O maser pumping, as was suggested previously (Wouterloot & Walmsley 1986), which also agrees with feasible pumping schemes (Elitzur et al. 1989).

Analysis of the IRAS colour–colour diagram of the sample does not provide any new information over that reported in Szymczak et al. (2002) and Beuther et al. (2002). Sources having different maser combinations are clustered in the reddest part of diagram corresponding to less evolved objects.

4. Conclusions

A high sensitivity survey of the H_2O maser line in an unbiased sample of 79 methanol maser sources resulted in 41 detections of which 28 are new. The water maser detection rate was 52%, which is comparable with the rates reported for samples of high-mass star-forming regions selected with other criteria mainly based on IRAS colours typical for UCHIIRs or radio continuum emission or/and thermal CS emission.

The sample was divided into four subsets, depending whether maser lines from OH, CH_3OH, and H_2O were observed in a source. Percentages of sources masing in two or three of the species or one only, as well as an association of maser and radio continuum and/or IR emission were analyzed, as well as the maser and IR luminosities.

We find that CH_3OH and H_2O evolutionary phases largely overlap and luminosities in both species are comparable. Only a small fraction ($\sim$10%) of CH_3OH/H_2O objects have OH emission detectable at the limits of current surveys.

In all subsets considered, the luminosity of the OH masers is lower than that of CH_3OH and H_2O masers. The evolutionary phase during which OH maser emission occurs seems to follow those with CH_3OH/H_2O emission, although an overlap of OH and CH_3OH maser phases seems to exist.

The lowest percentage of association with radio continuum was found for objects with CH_3OH masers alone, which seems to indicate that methanol masers (as H_2O masers) may trace objects that have not yet developed an ionizing core. At least one third of the H_2O masers in the sample have a velocity extent larger than 20 km s^{-1} suggesting their association with outflows or jets. For the majority of sources ($\sim$90%) the centroids of the OH and CH_3OH maser velocity intervals coincide to within 5 km s^{-1}. In contrast, for $\sim$40% of the H_2O sources the difference in the velocity centroids of H_2O and CH_3OH maser emission are larger than 10 km s^{-1}. Furthermore, the H_2O velocity centroids are blue-shifted relative to those of CH_3OH emission. These findings support previous suggestions that while CH_3OH masers originate from the innermost parts of the environments of high-mass protostars, high velocity features are unique to H_2O masers. These H_2O masers likely emerge from high velocity outflows driven by the central object and can persist at a greater distance from exciting source than CH_3OH masers.

The OH and CH_3OH maser luminosities are well correlated with the IR luminosity while the H_2O and IR luminosities are marginally correlated. These findings are fully consistent with pumping schemes of the three maser lines.

Acknowledgements. We thank T. K. Sridharan for providing maser data of his sample online. The work was supported by the KBN grant 2P03D01122.

References

Becker, R. H., White, R. L., Helfand, D. J., & Zoonematkermani, S. 1994, ApJS, 91, 347
Beuther, H., Walsh, A., Schilke, P., et al. 2002, A&A, 390, 289
Brand, J., & Blitz, L. 1993, A&A, 275, 67
Brand, J., Cesaroni, R., Comoretto, G., et al. 2003, A&A, 407, 573
Bronfman, L., Nyman, L. A., & May, J. 1996, A&AS, 115, 81
Caswell, J. L. 1996, MNRAS, 279, 79
Caswell, J. L., Vaile, R. A., & Forster, J. R. 1995, MNRAS, 277, 210
Charnley, S. B. 1997, ApJ, 481, 396
Charnley, S. B., Kress, M. E., Tielens, A. G. G. M., & Millar, T. J. 1995, ApJ, 448, 232
Churchwell, E., Walmsley, C. M., & Cesaroni, R. 1990, A&AS, 83, 119
Codella, C., Felli, M., & Natale, V. 1996, A&A, 311, 971
Codella, C., Lorenzani, A., Gallego, A. T., Cesaroni, R., & Moscadelli, L. 2004, A&A, 417, 615
Codella, C., & Moscadelli, L. 2000, A&A, 362, 723
Codella, C., Palumbo, G. G. C., Pareschi, G., et al. 1995, MNRAS, 276, 57
Cragg, D. M., Sobolev, A. M., & Godfrey, P. D. 2002, MNRAS, 331, 521
Elitzur, M., Hollenbach, D. J., & McKee, C. F. 1989, ApJ, 346, 983
Ellingsen, S. P., von Bibra, M. L., McCulloch, P. M., et al. 1996, MNRAS, 280, 378
Forster, J. R., & Caswell, J. L. 1989, A&A, 213, 339
Hofner, P., & Churchwell, E. 1996, A&AS, 120, 283
Kolpak, M. A., Jackson, J. M., Bania, T. M., Clemens, D. P., & Dickey, J. M. 2003, ApJ, 582, 756
Kurtz, S., Cesaroni, R., Churchwell, E., Hofner, P., & Walmsley, C. M. 2000, in Protostars and Planets IV, ed. V. Mannings, A. P. Boss, & S. S. Russell (Univ. of Arizona Press), 299
Menten, K. M. 1991, ApJ, 380, L75
Menten, K. M. 1996, Molecules in Astrophysics: Probes & Processes, IAU Symp., 178, 163
Menten, K. M., Reid, M. J., Pratap, P., Moran, J. M., & Wilson, T. L. 1992, ApJ, 401, L39
Minier, V., Ellingsen, S. P., Norris, R. P., & Booth, R. S. 2003, A&A, 403, 1095
Palla, F., Brand, J., Cesaroni, R., Comoretto, G., & Felli, M. 1991, A&A, 246, 249
Palla, F., Cesaroni, R., Brand, J., et al. 1993, A&A, 280, 599
Reid, M. J., & Moran, J. M. 1988, in Galactic and extra-galactic radio astronomy, ed. G. L. Verschuur, & K. I. Kellermann (Berlin: Springer)
Sewilo, M., Watson, C., Araya, E., et al. 2004, ApJS, 154, 553
Schutte, A. J., van der Walt, D. J., Gaylard, M. J., & MacLeod, G. C. 1993, MNRAS, 261, 783
Slysh, V. I., Val'tts, I. E., Kalenskii, S. V., et al. 1999, A&AS, 134, 115
Sridharan, T. K., Beuther, H., Schilke, P., Menten, K. M., & Wyrowski, F. 2002, ApJ, 566, 931
Szymczak, M., & Gérard, E. 2004, A&A, 414, 235
Szymczak, M., Kus, A. J., Hrynek, G., Kepa, A., & Pazderski, E. 2002, A&A, 392, 277
Szymczak, M., Hrynek, G., & Kus, A. J. 2000, A&AS, 143, 269
Valdettaro, R., Palla, F., Brand, J., et al. 2001, A&AS, 368, 845
van der Walt, D. J., Gaylard, M. J., & MacLeod, G. C. 1995, A&AS, 110, 81
van der Walt, D. J., Retief, S. J. P., Gaylard, M. J., & MacLeod, G. C. 1996, MNRAS, 282, 1085
Walsh, A. J., Hyland, A. R., Robinson, G., & Burton, M. G. 1997, MNRAS, 291, 261
Walsh, A. J., Burton, M. G., Hyland, A. R., & Robinson, G. 1998, MNRAS, 301, 640
Walsh, A. J., Bertoldi, F., Burton, M. G., & Nikola, T. 2001, MNRAS, 326, 36
Wood, D. O. S., & Churchwell, E. 1989, ApJ, 340, 265 (WC89)
Wouterlout, J. G. A., & Walmsley, C. M. 1986, A&A, 168, 237
Wyrowski, F., Schilke, P., Walmsley, C. M., & Menten, K. M. 1999, ApJ, 514, L43